Total-Count Calibration Blocks for use in uranium Exploration

Løvborg, Leif

Publication date:
1983

Document Version
Publisher's PDF, also known as Version of record

Risø-R-490

RISØ

Risø-R-490

Total-Count Calibration Blocks for Use in Uranium Exploration

L. Løvborg

Risø National Laboratory, DK-4000 Roskilde, Denmark
September 1983

RISØ-R-490

TOTAL-COUNT CALIBRATION BLOCKS FOR USE IN URANIUM EXPLORATION

L. Løvborg

Abstract. Transportable calibration blocks for field scintillometers and borehole probes were manufactured from concrete and installed at calibration sites in Denmark and Greece. The concrete mixes were prepared from aggregates of quartz sand and crushed uranium-thorium ore. Water-reducing agents and silica dust added to the cement paste produced concretes of acceptable porosity and pore structure. The content of ore was adjusted to provide block grades of approximately 2, 140, and 540 units of radioelement concentration (Ur). Thorium was estimated to contribute 0.39 ± 0.02 Ur per ppm Th. The adopted reference grades include concrete pore moisture and are normalized to an effective atomic number of 13. Grade instability due to radon emanation was not detected.

Experimental uncertainties stated in this report are estimated standard deviations.

INIS Descriptors. BOREHOLES; CALIBRATION; CALIBRATION STANDARDS; CONCRETES; EXPLORATION; SCINTILLATION COUNTERS; URANIUM

UDC 539.1.074.3 : 53.089 : 550.8 : 553.495

September 1983

Risø National Laboratory, DK-4000 Roskilde, Denmark

This work was done under Research Contract EXU-030-DK(G) between the Commission of the European Communities and Risø National Laboratory.

ISBN 87-550-0958-1
ISSN 0106-2846

Risø Repro 1983

CONTENTS

Page

1. INTRODUCTION

The portable scintillation counter began to replace the less sensitive Geiger-Müller counter around 1950 and has since become the most widely used field instrument in uranium exploration. It detects the gamma radiation from ^{214}Pb and ^{214}Bi in the ^{238}U decay series and is also sensitive to the gamma-ray emissions associated with the radioactivities of ^{235}U, ^{232}Th, and ^{40}K. For many years exploration geologists were not concerned about a unit of measurement that might be used for reporting the total content of radioelements in the ground. Most readings were taken on pure uranium mineralization and could be reported directly in terms of equivalent U_3O_8. In the nineteen-seventies exploration of low-grade uranium resources became intensified in several parts of the world, for instance in Greenland (Nielsen, 1981). This additional exploration made it necessary to allow for contributions to the instrument readings from ^{232}Th with daughters and, to a less extent, ^{40}K.

In 1976 the International Atomic Energy Agency issued the report "Radiometric reporting methods and calibration in uranium exploration" (IAEA, 1976). It established a unit of radioelement concentration which is based on the total-count response from an exploration target with 1 ppm U in radioactive equilibrium. This new total-count unit is becoming increasingly acknowledged as an adequate remedy for expressing scintillometer readings recorded on rock with mixed radioelement contents. The unit is generally known as the "Ur", a final abbreviation suggested by the OECD Nuclear Energy Agency (OECD, 1981). Converting a field reading into Ur is primarily a question of having access to sources of known total radioelement content. In effect, the success of the improved reporting standard will largely depend on the future availability of calibration sources at reasonable distances from the exploration sites.

The concrete blocks described here are transportable and have been developed as a possible starting point for a central supply

of reliable and inexpensive calibration sources which can be delivered to any desired destination. Scintillometer calibration blocks manufactured in this pilot study are similar to those developed by Bendix Field Engineering Corporation for the U.S. Department of Energy (Mathews and Kosanke, 1978). Furthermore, sources penetrated by a central hole have been manufactured for demonstrating the use of stacked concrete blocks for the calibration of borehole logging equipment. The main text of this report describes the materials used for the blocks and the tests and assays executed for establishing the radiometric block grades in an outdoor environment. It has been attempted to highlight the advantages of using water-reducing agents for decreasing the porosity of hardened cement paste. Another interesting aspect is represented by the use of a radioactive aggregate material containing both uranium and thorium. For convenience the more subtle details of the work done are presented in three short appendices.

2. DESCRIPTION OF THE BLOCKS

2.1. Dimensions and Radiometric Grades

The basic modules for establishing a surface calibration facility and a borehole model are shown in Fig. 1. An A-block is designed for mounting a scintillometer centrally on the top surface and consists of a 145 cm × 50 cm concrete well ring filled with more or less radioactive concrete. A B-block is 100 cm thick and equipped with a prefabricated hole from top to bottom. B-blocks manufactured for the pilot study have a hole diameter of 82 mm. By joining a series of differently loaded B-blocks together, a borehole model producing a stepwise-varying gamma-ray log can be constructed.

All blocks manufactured are based on three concrete types called L, M, and H. The radiometric in-situ grades of these source materials are presented in Table 1. L-concrete has an aggregate of

A - BLOCK

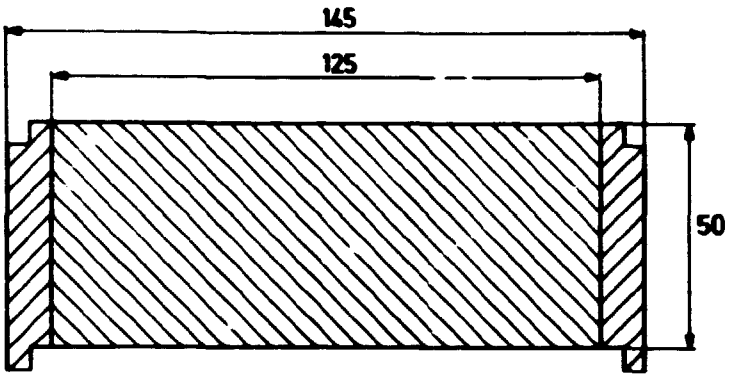

B - BLOCK

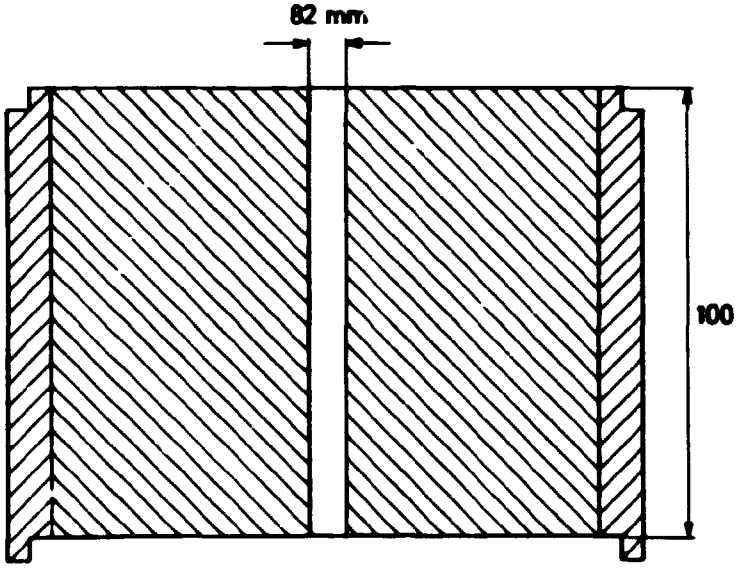

Fig. 1. Block modules for the calibration of field scintillometers and gamma loggers.

almost non-radioactive eocene quartz sand for obtaining a low background level in the instrument calibrations. H- and M-concrete is loaded with a radioactive aggregate containing uranium and thorium in a natural proportion of 1:2. Since 1 ppm Th is equivalent to approximately 0.4 ppm U (subsection 4.3), thorium contributes around 45% of the total grades. The latter are therefore less sensitive to radon emanation than the grades of pure uranium sources. Pure thorium sources without long-lived radon

Table 1. Radiometric in-situ grades for the concretes of the calibration blocks.

Concrete type	Content of radioactive material	Grade in Ur
L	Low	2.4 ± 0.2
M	Medium	139 ± 4
H	High	538 ± 15

gas have not been envisaged because of a 5% uncertainty on the uranium equivalent of thorium. Reference grades of 139 and 538 Ur accommodate exploration of uranium ore with grades of up to about 1000 Ur, but are insufficient for calibration of readings recorded with several thousand ppm U or Th.

2.2. Aggregate Materials

The radioactive aggregate for M- and H-concrete consists of crushed ore from the Kvanefjeld uranium deposit in Greenland. This deposit is situated at 61°N and 46°W in the Ilímaussaq alkaline complex and belongs to the category of disseminated, magmatic low-grade resources (Nielsen, 1981). Most of the uranium (and thorium) is contained in fine-grained lujavrites which are rocks consisting of microcline, albite, nepheline, arfvedsonite, aegirine, and a number of rare accessory minerals (Sørensen et al., 1974). The most abundant radioactive mineral is steenstrupine, a rare-earth phospho-silicate of mainly primary origin (Makovicky et al., 1980). Ore material for the blocks derives from a 960 m long adit driven into the centre of the deposit in 1979-80. The ore selected for crushing was so-called naujakasite lujavrite estimated to contain 369 ppm U and 809 ppm Th from 538 chip samples cut in the adit (Clausen, 1982).

Figure 2 shows the size distributions for quartz sand and ore particles which occur intermixed with each other in the M-con-

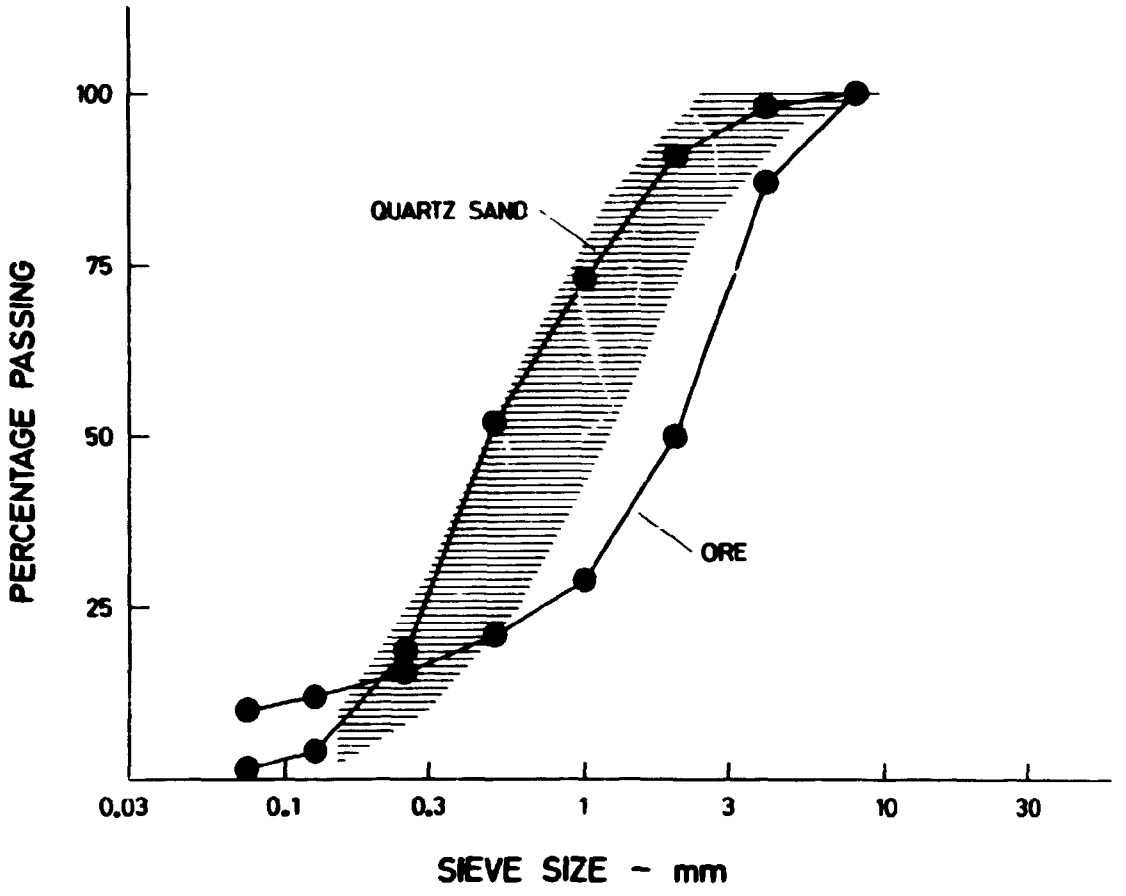

Fig. 2. Grading curves for the aggregate materials. Shaded area shows grading limits required by ASTM specification C33.

crete. The shaded area added in the figure represents the grading limits for fine aggregate required by ASTM specification C33 (Troxell et al., 1968). The quartz sand satisfies these grading limits, whereas the ore material is characterized by an undue contribution of crushing dust and other fine material. The many small ore particles are undesirable since they may be shaken out of the voids between the larger particles. They should be removed by screening in a possible future production of similar calibration blocks. It should be noted that the ore has been crushed to a maximum particle size of around 6 mm to suppress radioactive heterogeneity due to coarse particles.

Radioelement concentrations determined for dried samples of the aggregates and the cement type used are presented in Table 2.

Concentrations in % K, ppm eU, and ppm Th were assayed using sealed-can gamma-ray counting in three energy windows. As described in Appendix B, several reference materials were included for obtaining a confident eU and Th calibration of the counting equipment. Results in ppm U are based on neutron irradiations of 1-g splits followed by the counting of delayed fission neutrons from ^{235}U (Kunzendorf et al., 1980). These direct uranium determinations agree well with the measured eU contents, indicating that the ^{238}U in the ore and the other mix ingredients is in radioactive equilibrium. The resulting identity between eU and U is essential for the manufacture of total-count calibration blocks since ^{235}U delivers a count rate in excess of that produced by ^{214}Pb and ^{214}Bi in the decay series of ^{238}U.

Table 2. Radioelement contents of the major constituents of the blocks.

Material	% K	ppm U	ppm eU	ppm Th
Radioactive ore	1.9±0.6	399±8	419±8	851±13
Quartz sand	0.45±0.01	0.58±0.02	0.46±0.07	1.2±0.2
Portland cement	0.50±0.01	2.52±0.05	2.7±0.1	6.3±0.2

2.3. Mix Design and Manufacturing Process

Concrete mixes required to harden into material of good mechanical strength and low permeability must be amenable to compaction and contain as little water as possible per sack of cement. Adding surplus water to a mix for improving its workability renders the aggregate particles more liable to segregation and increases the porosity and permeability of the cement paste (Troxell et al., 1968; Neville, 1977; Fulton, 1964). Mixes of low water-cement ratios can be vibrated into uniform and coherent concretes through the use of various chemical admixtures which are finding increasing application in modern concrete manufacturing practice (Rixom, 1978). The mixes for the blocks have

water-cement ratios smaller than 0.55 by virtue of air-entrainment and the addition of a superplasticizer. Furthermore, they contain a quantity of silica dust for reducing the porosity of the cement paste.

The proportioning of the mixes, based on workability tests with 10-l trial batches, is presented in Table 3. L-mix required the least amount of water because the quartz sand was moist and consisted of rounded particles. A greater quantity of water per m^3

Table 3. The proportioning of the concrete mixes.

Mix ingredient	kg/m^3		
	H	M	L
Crushed ore	1785	402	-
Quartz sand	-	1324	1767
Portland cement	300	300	325
Silica dust	24	24	26
Air-entraining agent	0.16	0.16	0.18
Superplasticizer	4.9	4.9	5.0
Tap water, ca.	160	160	90
Total	2274	2215	2213

of mix was necessary to wet the surfaces of the irregular ore particles in H- and M-mix. The action of an air-entraining agent is that of reducing the surface tension of the water whilst introducing a number of tiny air bubbles in the mix. This entrained air, supplied in amounts of about 80 l/m^3 to mixes prepared from fine aggregate, is different from the air unintentionally entrapped as large bubbles during mixing and batching operations. The microscopic voids left in air-entrained, hardened concrete are shown on photographs in subsection 3.1. They increase the frost resistance of the calibration blocks by acting as a reservoir for ice expansion (Rixom, 1978).

The mixes were prepared by means of a non-tilting drum mixer designed for a batch volume of 100 l. A uniform blending of the mix ingredients was obtained by rotating the batches for at least three minutes before they were discharged. The use of a superplasticizer as an admixture made the mixes very suited for compaction with a poker vibrator in their circular containments. All blocks manufactured were dressed with insulating material for preventing the development of cracks during the setting times.

2.4. Calibration Facilities

A- and B-blocks weigh around 1900 and 3800 kg, respectively. They are supplied with eye bolts and can rather easily be moved and positioned with a crane truck. A scintillometer calibration station is based on the block series AL-AM-AH from which the count rate per Ur can be determined by plotting the block readings against the grades in Table 1. A suitable borehole model is obtained by stacking the series BH-BL-BM-BL in that succession. This configuration produces two symmetrical logging peaks with flat plateaus and steep flanks. By coating the joining faces of the B-blocks with a layer of plastic padding, the calibration hole can be made watertight for the determination of calibration factors in a water-filled hole.

Complete calibration facilities like these have been established at Risø National Laboratory and the Nuclear Research Centre Demokritos at Aghia Paraskevi in Athens, Greece. As shown in Fig. 3, the blocks AH-1, AL-2, and AM-3 installed at Risø are close to an array of six larger sources, UT-1 to U-1. These larger sources are primarily intended for the calibration of gamma-ray spectrometers and were described by Løvborg et al. (1981). Figure 4 shows the execution of a counter calibration on the A-blocks which are placed in the ground both at Risø and Demokritos. The borehole model at Risø is presented in Fig. 5. It is kept on the surface, which implies that the probes must be immersed from a narrow working space 4 m above the ground. At Demokritos the similar model is installed in a pit providing a calibration hole in flush with the ground (Fig. 6).

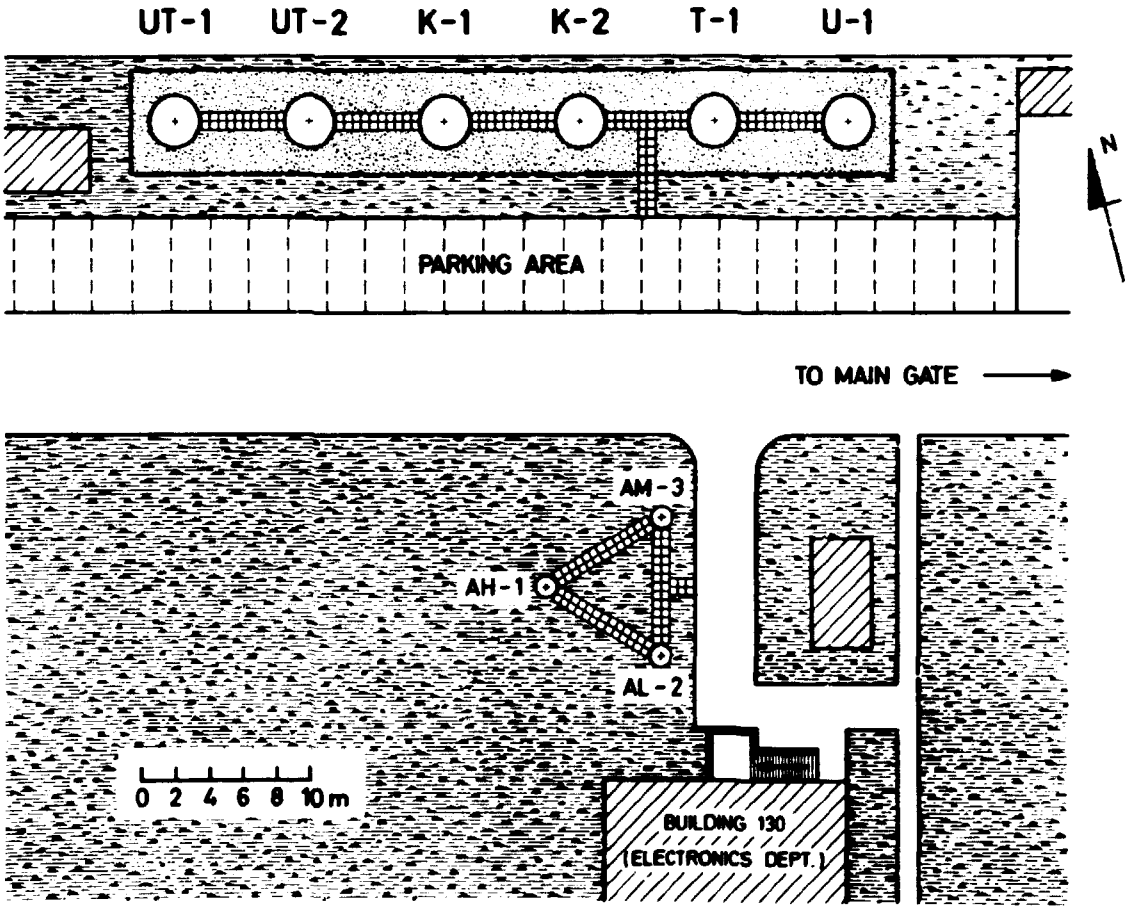

Fig. 3. Siting of scintillometer calibration blocks AH-1, AL-2, and AM-3 at Risø National Laboratory. The larger sources UT-1 to U-1 are used for spectrometer calibrations and were described by Løvborg et al. (1981).

Fig. 4. Calibration reading with field scintillometer on A block.

Fig. 5. Borehole calibration model errected at Risø by stacking blocks BH-1, BL-2, BM-3, and BL-4. Logging probe ready for immersion is seen on the top platform. Water supplied to the calibration hole can be emptied through a tube in the ground.

Fig. 6. Calibration of portable gamma logger in borehole model installed at the Nuclear Research Centre Demokritos in Athens. The model is contained in a concrete-lined pit and has the same configuration as the model at Risø.

3. CONCRETE TESTING RESULTS

Concrete stored in a natural environment absorbs water vapour that may condense or freeze in the porespaces depending on the temperature and humidity of the surroundings. The moisture supplied to a calibration block lowers its radiometric grade and affects the internal emanation and migration of radon gas. This complicating factor has been assessed from various tests on drill core from the blocks and samples of the mixes. A freeze-thaw test for estimating the durability of the concretes has also been performed.

3.1. Porosity and Air-Pore Structure

Figures 7 to 10 are pictures from a microscopic examination of drill-core thin-sections that have been impregnated with a fluorescent substance for obtaining an enhanced image of the concrete porosities. Figures 9 and 10 (H-concrete) are fluorescence recordings, while Figs. 7 and 8 (L- and M-concrete) were recorded with parallel nicols and without fluorescence for getting the best impression of the shape of the aggregate particles. The circular inclusions seen on all the pictures are entrained air. As a rule, the porosity of the cement paste is quite low and similar to that of a paste without embedded silica dust and a water-cement ratio of about 0.40. H-concrete is the most porous source material, as estimated from the density of the paste and the total number of microscopic cracks. This is substantiated by the fissured ore particles in Fig. 9 and the cracks seen in Fig. 10. In general, it is difficult to make a highly impermeable concrete from crushed aggregate due to the fissures produced by the crusher mill and the thinning of the cement paste along the surface of angular particles. The cracks in Fig. 10 are ascribed to plastic initial setting of the mix. Signs of internal bleeding in H-concrete have also been observed.

Table 4 provides an impression of the air-pore structure of the blocks. These data were recorded using computerized image scanning of cut and contrast-impregnated core sections (Christensen et al., 1979). The blocks contain very little entrapped air, as seen from the small number of pores greater than 2 mm. Most of the smaller pores were supplied through the air entrainment of the mixes and are characterized by a satisfactorily low spacing factor of 0.10 to 0.13 mm. The rather small pore content of H-concrete indicates an ineffective action of the air-entraining agent in a mix prepared from crushed ore without quartz sand.

Fig. 7. L-concrete (x 63, parallel nicols). Cement paste with quartz grains and circular inclusions of entrained air.

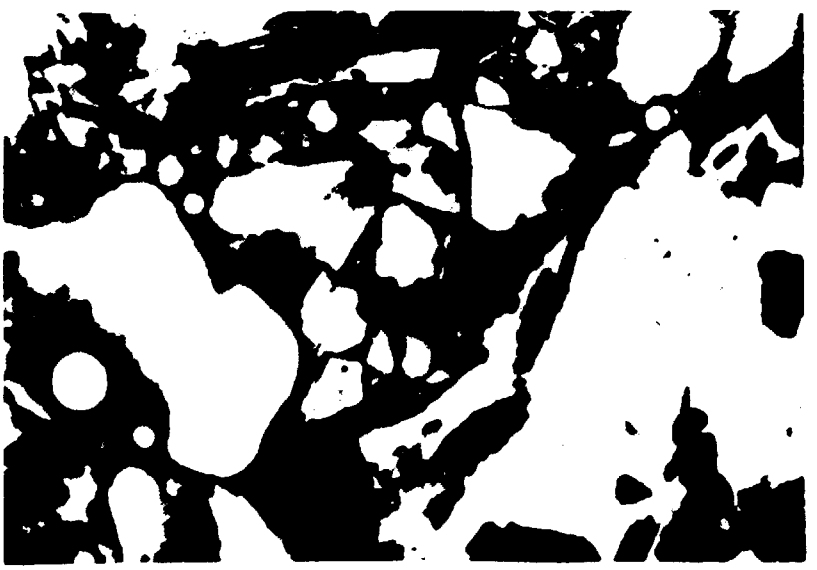

Fig. 8. M-concrete (x 63, parallel nicols). Larger irregular ore particle in cement paste with grains of quartz and ore.

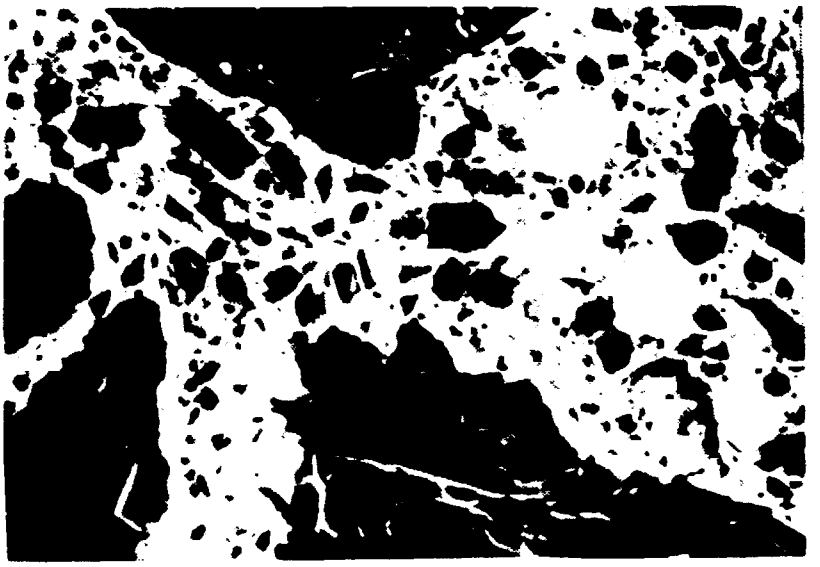

Fig. 9. H-concrete (x 63, fluorescence). Dense cement paste with accentuated porosities. Micro-fissures are seen in the large ore particles.

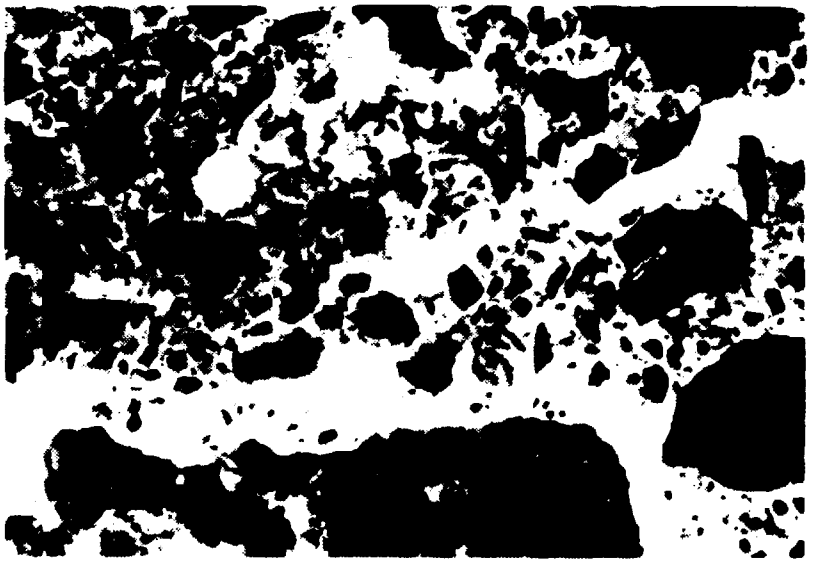

Fig. 10. H-concrete (x 63, fluorescence). Cement paste with irregular cracks due to plastic initial setting of the mix.

Table 4. Amount and distribution of air pores in the concretes (determined according to ASTM specification C457).

Concrete	Pore content (%)		Specific surface (mm^2/mm^3)	Spacing factor (mm)
	>7.5 μm	>2 mm		
L	11	1	23	0.12
M	10-11	1-2	21	0.13
H	4-9	0.2-1	43	0.10

3.2. Moisture Absorption and Total Porosity

The penetration of moisture into the blocks was estimated by immersing a set of core samples in water and following the resulting weight increases with time. Saturation was invoked after 30 days by first drying the samples and then soaking them in vacuum. Table 5 shows the result of this simple test. The water absorption was fast on the first day and slowly reached 75 to 80% of the saturation limit. The inability of a small sample to saturate over a prolonged period of time suggests that the blocks never become saturated with water in their natural surroundings. The saturation densities in Table 5 were measured by weighing the saturated samples in air and water. The weights of the samples

Table 5. Water absorption, saturation density, and total porosity for concrete core samples.

Concrete	Percent saturation		Saturation absorption	Saturation density	Total porosity
	1 day	30 days	(%)	(g/cm^3)	(%)
L	60	75	6.0 - 6.5	2.17	12 - 13
M	70	80	6.2 - 6.9	2.23	13 - 14
H	70	75	8.6 - 11	2.34	19 - 23

when they were dry furthermore provided the total porosities of the concretes. L- and M-concrete is only slightly more porous than expected from the content of air pores (Table 4). For H-concrete the porosity is much greater than that contributed by entrained and entrapped air, an additional indication of cracks and weak areas in the cement paste.

3.3. Freeze-Thaw Test

A freeze-thaw test was performed with sawn concrete prisms alternatively kept in a saturated salt solution at -15°C and flushed with running water at 20°C. No length alternations were detected after 250 of these temperature cycles. The test indicates that the blocks are durable and suited for installation in places with a severe climate.

3.4. Radon Emanation

Radon (^{222}Rn) emanated by an ore particle in concrete migrates through the capillaries and voids in the cement paste and may deposit its decay products at a distance from the particle. In this way the concentrations of ^{214}Pb and ^{214}Bi in a calibration block may become progressively diminished in the direction of the block surface which forms an exit for the migrating radon atoms. The net result is a smaller radiometric grade and an associated calibration error.

The amount and mobility of the radon in a calibration block is controlled by the emanation power of the aggregate particles and the pore structure and moisture content of the concrete. The steenstrupine carrying the uranium of the ore selected for this study is metamict or altered (Makovicky et al., 1980), a feature that increases the escape probability for the interstitial radon atoms in the crystals (Barretto, 1975). Also, the ore-crushing produced particles with cracks plus many small particles of large specific surface. As a result the block contents of radon outside the ore aggregate might be prominent. The mobility of

unbound radon in concrete is a combined result of migration by diffusion and movements invoked by atmospheric pressure drops. Culot et al. (1976) determined a relaxation distance of about 10 cm for radon diffusing from mill tailings through a concrete wall with assumed porosities of 5 and 25%. Pore moisture shortens the diffusion distance very significantly (Tanner, 1964; Tanner, 1980). A coherent air-pore structure provides space for collective radon movements towards the surface of a concrete structure. In the air-entrained concrete used for the blocks radon cannot flow easily since the pores are not connected with each other.

To test the emanation power of M- and H-concrete, samples of the mixes were ground to -100 mesh and dissipated in 20-cm glass dishes for obtaining a large emanating surface. The fractional radon losses after a prolonged storage of the sample material in a dry place were determined by enclosing 250 g of material in metal cans and recording the ^{214}Bi activity of the samples as a function of time. This assay method is described in Appendix C. Similar surfaces for the testing of emanation were produced from uranium-loaded materials U-1, UT-1, and UT-2 of the spectrometer calibration sources at Risø National Laboratory (Fig. 3). These latter materials, especially the U-1, have been suspect of radon emanation for a long time because their eU in-situ concentrations are more or less anomalous (Appendix A).

The result of this extended assay is shown in Table 6, third column. Radon losses were detected only for samples U-1 and UT-1. It was thereafter attempted to enhance the emanation by exposing the materials to a humid atmosphere for one month. Moisture increases the emanation power by preventing the escaping radon atoms from becoming attached to the emanating particles (Tanner, 1980). Table 6 shows that the effect of moistening and drying the materials was quite distinct. From this repeated trial, material U-1 is identified as the strongest emanator. The emanation from UT-1 and UT-2 is smaller, though significant, while moisture supplied to H-concrete produces a barely detectable emanation. The suggested contents of loosely bound radon in the spectrometer calibration sources can be explained by an exclus-

Table 6. Radon emanation from powder samples of uranium-loaded source materials.

Source material	ppm U	Emanation power (%)	
		Dry material	Material with 3 to 7% moisture before drying
U-1	230	5	18
UT-1	57	4	5
UT-2	20	n.d.	11
M concrete	80	n.d.	n.d.
H concrete	350	n.d.	3

ive use of very fine ore particles for the mixes. The latter were sand-cement mortars, which are materials that cannot be compacted properly due to the absence of a stony aggregate. Figure 11 shows the microscopic structure of one of the sources, U-1, a notorious radon emitter that may lose up to forty percent of its gamma radiation (Løvborg et al., 1978). The pore structure is extremely open and easily permits a release of outflowing radon gas.

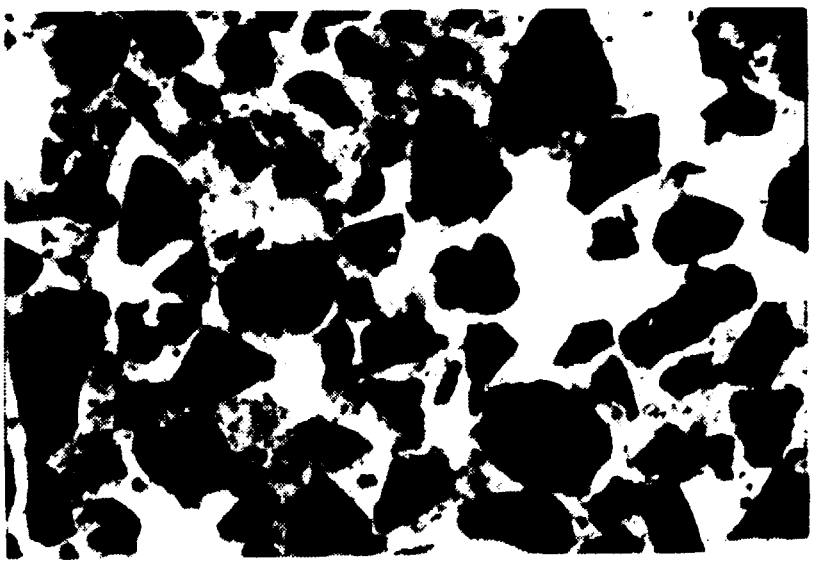

Fig. 11. Source material U-1 (x 63, fluorescence). Sand-cement mortar with embedded tiny particles of pitchblende. The large inclusions of entrapped air are more or less coherent and form an exit passage for radon emanated by the ore particles.

4. GRADE ASSIGNMENT

The radiometric block grades in Table 1 have been determined by adding the grades supplied separately by uranium, thorium, and potassium. For obtaining the grade contributions from Th and K, it was necessary to assess the Ur correspondents of 1 ppm Th and 1% K. This has been done from the combined use of detector response calculations and total-count calibration of small detectors with the sources UT-1 to U-1. Improved eU concentrations for these sources were evaluated before the present study (Appendix A); the new reference contents make it possible to record the count rate from 1 Ur in spite of the radon emanating from the sources. A further complication in the assignment of block grades arose from the need to estimate the grade diminuation due to pore moisture and iron contained in the ore aggregate.

4.1. The Outset: Radioelement Concentrations per Dry Weight of Concrete

A block absorbing w% moisture gets its radioactive concentrations diminished by a factor of $1/(1+w/100)$. If w can be estimated, the in-situ concentrations are derivable from an assay of the radioelement contents per dry weight of concrete.

The assay results for dry concrete presented in Table 7 are based on L, M, and H composite samples prepared from hardened and finely ground mixture lumps. Five 250-g splits of each composite sample were dried for 24 h at 110°C and sealed in metal cans. They were counted twice after a normally observed radon build-up period of one month. Individually assayed radioelement contents were very uniform; for H- and M-concrete it was possible to estimate the mean concentrations of eU and Th with a precision of 1%. The overall uncertainties stated in Table 7 include the random assay error as well as the accuracy obtainable with the counting standards (Appendix B).

Since practically all the uranium-thorium content of H- and M-concrete is contributed by ore aggregate, the assay suggests a value of between 4.30 and 4.33 for the ratio between the ore contents of these materials. The mixes were actually loaded with ore in a proportion of 4.33:1 by weight (derivable from Table 3). This excellent correspondence may be taken as evidence that the composite samples were fully representative of the mixes.

Table 7. Radioelement contents per dry weight of concrete.

Concrete	% K	ppm eU	ppm Th
L	0.43 ± 0.02	1.00 ± 0.08	2.4 ± 0.2
M	0.79 ± 0.04	80.0 ± 1.5	164 ± 3
H	2.0 ± 0.1	346 ± 6	706 ± 11

4.2. Assay of Pore Moisture

Moisture absorbed by the blocks in their natural surroundings might have been determined with a neutron moisture gauge. The use of such a device was not recommended because of the risk of getting the blocks activated for a period of time. Instead it was attempted to assay the pore moisture by monitoring the A-blocks at Risø and Demokritos with a portable gamma-ray spectrometer. The philosophy of this approach is explained by the following procedure and results:

A Geometrics model GR-410 spectrometer was calibrated on the sources UT-1 to U-1 using 2 x 2 and 3 x 3 in. NaI(Tl) scintillation detectors. This was done with and without a thick lead shield serving as a collimator for the detectors. Each of the calibration runs provided a set of stripping ratios and sensitivity factors for measuring the approximate in-situ radioelement contents of an A-block. Monitoring with a shielded detector required no modification of the experimental procedure.

When the detectors were unshielded, the sensitivity factors were reduced in a proportion of $(1-2h/d_1)/(1-2h/d_2)$ with d_1 = 125 cm (the effective diameter of an A-block) and d_2 = 300 cm (the diameter of the calibration sources); h is the distance from the surface to the centre of the detector crystal. This reduction factor is based on a simple geometric consideration (Løvborg, 1982).

The recorded eU and Th contents in AH- and AM-blocks are listed in Table 8. These determinations are differential with respect to the AL-blocks of the two calibration facilities. It is not possible to see any significant difference between the results for blocks at Risø and Demokritos. The variability shown by the

Table 8. Monitored in-situ radioelement concentrations in AH- and AM-blocks.

Month/year	Place	Detector (inches)	Shielding	AH less AL		AM less AL	
				ppm eU	ppm Th	ppm eU	ppm Th
07/82	R	3 x 3	+	335	654	78.7	150
09/82	R	2 x 2	-	306	672	71.9	160
11/82	R	2 x 2	-	309	651	72.0	158
11/82	R	2 x 2	+	332	653	80.3	155
11/82	R	3 x 3	-	318	621	75.0	151
11/82	R	3 x 3	+	319	647	75.0	155
02/83	R	3 x 3	-	318	613	74.8	150
04/83	R	2 x 2	-	334	632	77.2	154
04/83	D	2 x 2	-	339	666	81.4	160
04/83	R	3 x 3	-	319	663	75.6	157
04/83	D	3 x 3	-	330	697	75.7	156
04/83	R	3 x 3	+	326	635	76.0	153
04/83	D	3 x 3	+	321	648	76.6	156
04/83	R	3 x 3	-	318	614	75.6	149
Mean value				323	648	76.1	155
Coefficient of variation				3.0%	3.6%	3.5%	2.3%

R = Risø

D = Demokritos

observations appears to be random and about the same for uranium and thorium. Since there is no detectable correlation between the readings and the time of the year, the moisture contents of the blocks cannot vary much with season.

A first attempt to assess the block moisture, w, is presented in Figs. 12 and 13. Here the laboratory assays from Table 7 are plotted against the concentration differences determined by monitoring. If w were the same for H- and M-concrete, both plots should furnish a straight line with a slope of 1+w/100. Actually, the large uncertainties of the estimated regression slopes do not support an assumption of identical moisture contents in the concretes. The interesting feature of Figs. 12 and 13 is their similarity. Th and eU regression slopes deviating by less than two percent from each other confirm the validity of the calibration of the portable spectrometer and suggest that no radon is escaping from the blocks.

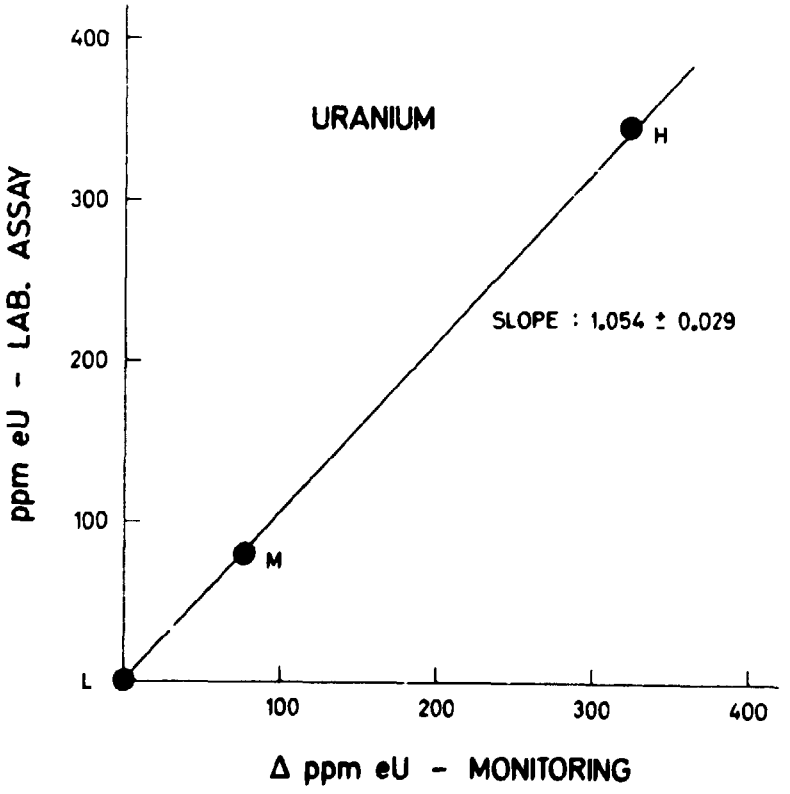

Fig. 12. Plot of eU laboratory assays and eU concentration differences determined by radiation monitoring of A-blocks.

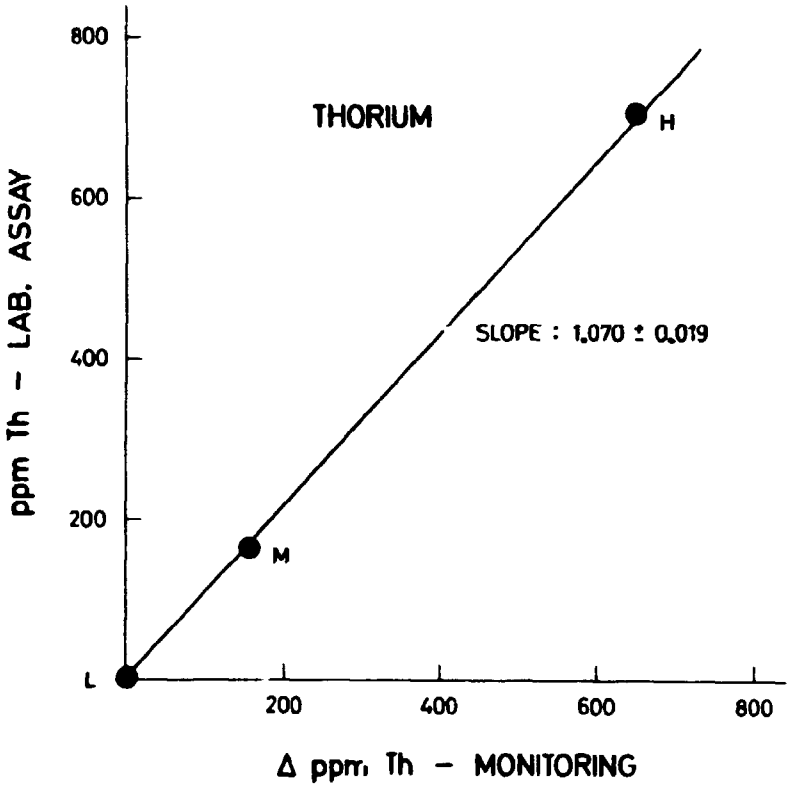

Fig. 13. Th plot similar to Fig. 12.

Table 9 shows the result of processing the experimental data for H- and M-concrete separately. From this comparison of laboratory assay and monitoring it is quite clear that AH-blocks contain more moisture than AM-blocks. Since the saturation absorption of the concretes is known with reasonable accuracy (Table 5), it is possible to convert the separately calculated moisture contents into a corresponding degree of saturation. A saturation factor of 0.7 was adopted and used for assigning pore moisture to all blocks manufactured; these inferred moisture contents are shown in Table 13 in subsection 4.4. The corresponding in-situ radio-element concentration are presented in Table 10. Since the ^{238}U in the blocks appears to be in equilibrium with its gamma-ray emitting daughters, ppm U is a relevant unit for reporting the radiometric uranium contents of the blocks.

Table 9. Moisture contents in A-blocks suggested by the radioelement concentrations in Tables 7 and 8.

Radioelement	Lab. assay conc./monitored conc.	
	AH	AM
U	1.068	1.038
Th	1.086	1.049
Average	1.077 ± 0.009	1.044 ± 0.005
Moisture content (%)	7.7 ± 0.9	4.4 ± 0.5
Corresponding degree of saturation	0.79 ± 0.13	0.67 ± 0.08

Table 10. Estimated in-situ radioelement concentrations for the blocks.

Concrete	% K	ppm U in equilibrium	ppm Th
L	0.41 ± 0.02	0.96 ± 0.08	2.3 ± 0.2
M	0.76 ± 0.04	76.5 ± 1.5	157 ± 3
H	1.9 ± 0.1	324 ± 6	660 ± 11

4.3. Uranium Equivalents of Thorium and Potassium

In principle the concentration of uranium that produces the same count rate as 1 ppm Th or 1% K can be calculated from the emission rate of gamma rays per gram of radioelement. Potassium is easy to deal with since ^{40}K is a monoenergetic emitter with a specific yield of 3.30 photons/s per g K. For uranium and thorium the calculation of detector count rates is rendered difficult by the complex line spectra of ^{238}U, ^{235}U, and ^{232}Th with respective daughters. The computational result presented here is based on the gamma- and X-ray energies and intensities contained

in the last updated version of the Evaluated Nuclear Structure Data File of the Oak Ridge Nuclear Data Project (see, for example, NCRP, 1978). Another complexity that must be coped with is the large number of scattered gamma rays contributed by an extended source medium. The computer programs GAMP1 and GFX developed by Kirkegaard and Løvborg (1979) made it possible to calculate the detailed flux energy distribution over an infinite source. By incorporating the decreasing efficiency of a small NaI(Tl) detector with increasing gamma-ray energies, the count rates from 1 ppm U, 1 ppm Th, and 1% K could be predicted and their ratios formed. It was even possible to include the effect of the uncertainties of the gamma-ray intensities used in the calculation. This was done by perturbing the single emissions and recording the resulting standard deviation from a number of repeat runs.

The result stated in the first line of Table 11 was calculated for a source medium of granite. Calculations for other source media have shown that the chemical compositions of these virtually have no effect on the recorded uranium equivalents. Also, it does not matter that the source dimensions are infinite. The adjoint Monte-Carlo code GAMO mentioned by Løvborg et al. (1981) furnishes almost identical results for source diameters of between 1 m and infinity. The estimate of 0.41 + 0.01 Ur per ppm Th is considerably smaller than that derived from the older emission data of Beck (1972) and reported by Løvborg et al. (1976). A value of 1.000 Ur per ppm U follows from the definition of 1 Ur and is merely included to show the contributions from ^{238}U and ^{235}U.

The experimental uranium equivalents in Table 11 are from calibration results for 1 1/2 x 1 and 2 x 2 in. detector crystals. The calibration, performed with the sources UT-1 to U-1, was repeated for various energy thresholds in the range from 30 to 200 keV. Individual results from this trial are shown in Appendix A. The measured Ur correspondents of 1 ppm Th were all fairly close to the computational value and justified the adoption of a final estimate based on calculation plus experiment. For potassium the experiment demonstrated a distinct increase in the number of Ur

Table 11. Evaluation of uranium equivalents for the assignment of block grades.

	Uranium equivalent (Ur)				
			1 ppm U		
	1 ppm Th	1% K	^{238}U	^{235}U	Total
Calculated	0.41 ± 0.01	1.22 ± 0.02	0.965	0.035	1.000
Experimental	0.37 ± 0.01	1.10 ± 0.20			
Adopted	0.39 ± 0.02	1.10 ± 0.20			1.000

recorded with increasing detector dimensions and threshold settings. This effect was not derived from the calculation which was executed for a 1 1/2 x 1 in. detector and an energy cut-off of 30 keV. The adopted Ur correspondent of 1% K matches typically used counter thresholds of 30 to 100 keV and has an associated relative uncertainty of about 20 percent. This low precision is unimportant because of the small potassium contents of the blocks. Conversely, the difficulty of specifying an exact translation of K concentrations into Ur seems to prohibit the use of potassium for the construction of total-count calibration sources.

4.4. Correction for Z-effect

The large ore content in H-concrete makes the gamma-ray attenuation of this material slightly greater than the attenuation of L- and M-concrete. The effect primarily consists in the absorption of low-energy gamma rays by iron in the ore and can be described by an enhanced effective atomic number (Kogan et al., 1969). It is therefore necessary to use separate grade conversion factors for each concrete type. For M-concrete the uranium equivalents in Table 11 have been used as they are, while the corresponding conversion factors for L- and H-concrete have been adapted to a Z_{eff} equal to that of M-concrete. The corrected

conversion factors are based on detector response calculations for A-blocks with the GAMO code which accommodates cylindrical detector-source geometries.

Chemical compositions ascribed to the blocks in the response calculations are shown in Table 12. The chemical data originate from an XRF assay of the composite samples of the mixes. To get the content of H_2O, the total percentage of oxides exclusive of H_2O was equated to the percentage of dry mix ingredients. The

Table 12. Chemical compositions of the concretes.

Oxide	Percent abundance		
	L	M	H
SiO_2	76.7	69.9	44.7
TiO_2	0.2	0.2	0.2
Al_2O_3	1.9	4.0	11.0
Fe_2O_3	0.6	2.9	10.2
MnO	0.0	0.1	0.6
MgO	0.1	0.1	0.2
CaO	8.6	8.3	9.5
Na_2O	0.1	2.2	9.5
K_2O	0.5	0.8	2.1
H_2O *)	11.2	11.3	11.4
P_2O_5	0.1	0.2	0.6
	100.0	100.0	100.0

*) Consumed mix water plus pore moisture.

mix water (including the moisture in the quartz sand) plus the pore moisture could then be incorporated in the series of block constituents. Resulting effective atomic numbers are added in Table 13 which summarizes the important physical characteristics of the blocks. The in-situ densities are required in response calculations applied to sources of finite dimensions. They follow from the saturation densities in Table 5 and the assumed saturation factor of 0.7. Table 14 contains the corrected grade

Table 13. Estimated pore moistures, in-situ densities, and effective atomic numbers.

Concrete	Pore moisture (%)	Density (g/cm^3)	Z_{eff}
L	4.4	2.13	12.5
M	4.6	2.19	13.0
H	6.9	2.28	14.6

Table 14. Factors for converting the in-situ radioelement concentrations into block grades.

Concrete	Ur		
	1% K	1 ppm U	1 ppm Th
L	1.13 ± 0.21	1.03 ± 0.01	0.40 ± 0.02
M	1.10 ± 0.20	1.00 ± 0.00	0.39 ± 0.02
H	1.01 ± 0.20	0.92 ± 0.01	0.36 ± 0.02

conversion factors for L- and H-concrete. Adopting the M-concrete as a base of reference corresponds to a normalization of all the block grades to a common effective number of 13.0.

This last step finishes the procedure needed for estimating the radiometric grades of total-count calibration blocks that are loaded with uranium and thorium and contain different amounts of pore moisture. The final block grades, derived by combining the data in Tables 10 and 14, were introduced at the beginning of this report (Table 1) in order to stress their character of a final result.

5. GRADE CONTROL

The monitoring trials and response calculations reported in the preceding section were exclusively performed with A-blocks as targets. B-blocks have been incorporated in two additional experiments set up for demonstrating the reliability of the estimated grades.

In the first experiment, the borehole model at Risø was logged with a Mount Sopris model-1000 gamma logger with an attached scaler. The probe of this logger houses a 1/2 x 1 1/2 in. NaI(Tl) detector. A log recorded in steps of 10 cm with water in the hole is presented in Fig. 14. Five single readings on the plateaus of the logging peaks from BH-1 and BM-3 were averaged for use in a plot of count rate versus grade. The background was read from the log of BL-4; use of BL-2 was not attempted since the log of this block contains a small radiation contribution from the adjoining blocks, BH-1 and BM-3. Figure 15 shows the resulting calibration plot. The three data points are essentially positioned on a straight line, indicating that the ratio of grade H- to M-concrete is reliable. If the Z-correction of the grade conversion factors for H-concrete had not been applied, the data point for BH-1 would have moved 45 Ur to the right with a resulting loss of experimental linearity. The Mount Sopris gamma logger was previously calibrated in boreholes drilled in the rocks of the Kvanefjeld uranium deposit from where the ore for the blocks was supplied. This old calibration was based on the radioelement contents in dry drill core and resulted in a calibration factor of 2.24 ± 0.15 counts/s per ppm U (Løvborg et al., 1972). The greater factor of 2.57 ± 0.05 counts/s per Ur recorded with the borehole model may partly be explained by the use of moisture-corrected reference grades for the blocks.

In the seocnd experiment, the borehole models at Risø and Demokritos were logged with a 2 x 2 in. detector connected to a GR-410 portable spectrometer. Plateau count rates recorded in

the total-count window are shown in Table 15. The two borehole models produce identical count rates within the limits set by counting statistics. This result plus that of monitoring the A-blocks (Table 8) suggest that blocks manufactured from identical mixes have identical grades.

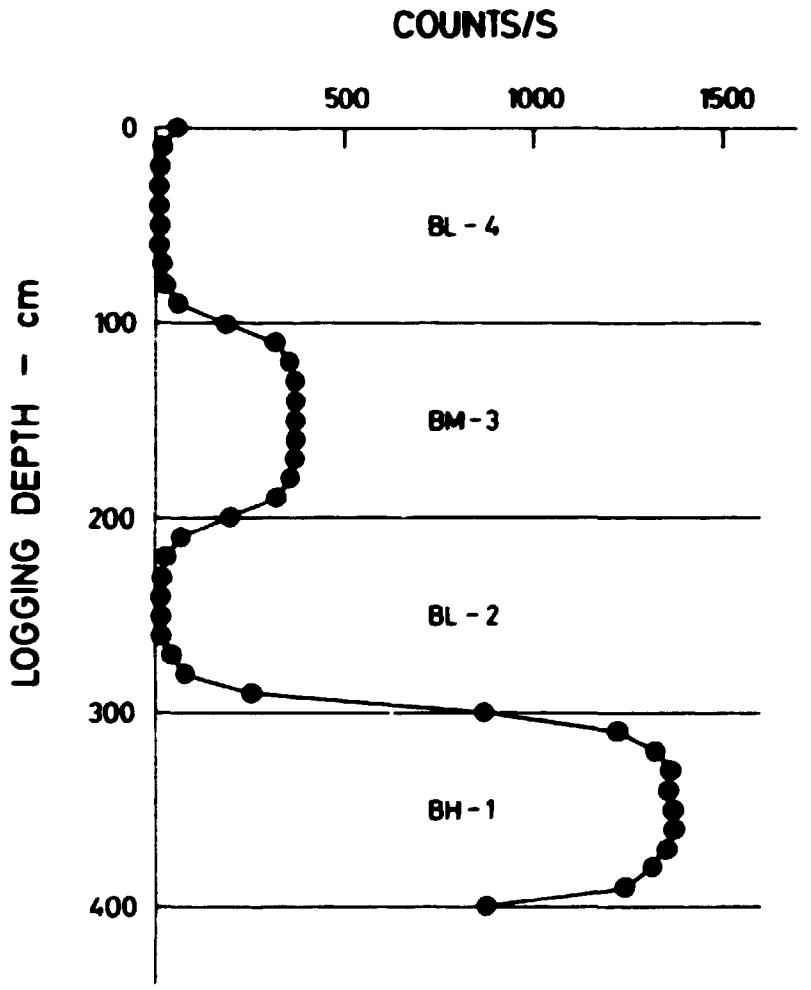

Fig. 14. Gamma-ray log recorded in the borehole model at Risø with water in the hole.

Table 15. Plateau count rates measured in borehole models with 2 x 2 in. detector (0.5 - 0.8 MeV).

Risø		Denokritos	
Block	Counts/s	Block	Counts/s
BL-4	43 ± 4	BL-8	43 ± 5
BM-3	444 ± 5	BM-7	447 ± 3
BL-2	63 ± 20	BL-6	71 ± 30
BH-1	1735 ± 22	BH-5	1722 ± 13

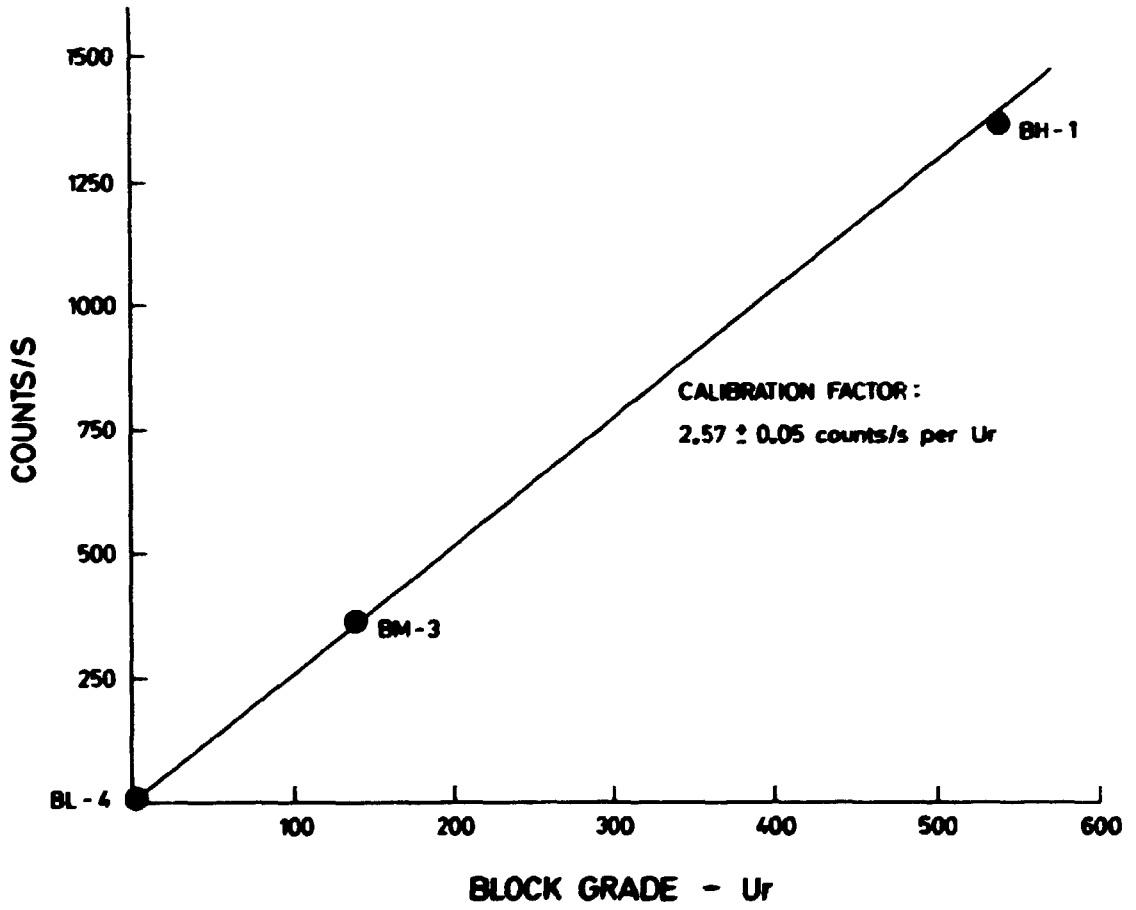

Fig. 15. Calibration line obtained from the log in Fig. 14.

6. CONCLUSION

This study has demonstrated that concrete calibration blocks of uniform grades can be manufactured centrally for distribution among users in various countries. The transportation cost involved in setting up a scintillometer calibration facility or a borehole model far away from the production site is offset by a great saving of time and effort for the user who might consider a manufacture of sources from locally available ore material. The ore used for the blocks described here may not be the best choice because of the limited calibration grade obtainable with it. Actually, the blocks having Kvanefjeld lujavrite as the only aggregate are rather inadequate due to their increased moisture absorption and enhanced effective atomic number. An aggregate of ore particles intermixed with quartz sand produced an acceptable source material at the expense of grade. If an ore of greater radioelement content and similar small emanation power could be provided, much of the experience obtained in this study could be used for starting a production of calibration blocks of elevated grades.

ACKNOWLEDGEMENTS

The financial support from the Commission of the European Communities is greatly appreciated. The blocks were made at the laboratory of H. Hoffmann & Sønner A/S; Sven Borgselius proposed the use of concrete additives and proportioned the mixes. Arne Damgård Jensen of Teknologisk Institut supplied most of the concrete testing results. The in-situ measurements were executed by Erling Johannsen who spent much time freezing outdoors at Risø, but recovered in Athens. Anne Marie Eichen, Lene Wittrock and Kirsten Hansen typed the manuscript, and Ellen Jensen made the drawings. Special thanks are due to George Sideris of the Greek

Atomic Energy Commission for his co-operation and hospitality in connection with the establishment of a calibration facility at the Demokritos Research Centre.

REFERENCES

AUSTIN, S.R. (1975). A laboratory study of radon emanation from domestic uranium ores. Radon in uranium mining (International Atomic Energy Agency, Vienna) 151-163.

BARRETTO, P.M.C. (1975). Radon-222 emanation characteristics of rocks and minerals. Radon in uranium mining (International Atomic Energy Agency, Vienna) 129-150.

BECK, H.L. (1972). The absolute intensities of gamma rays from the decay of ^{238}U and ^{232}Th. HASL-262, 14 pp.

CHRISTENSEN, P., GUDMUNDSSON, H., THAULOW, M., DAMGÅRD JENSEN, A. and CHATTERJI, S. (1979). Struktur- og bestandelsanalyse af beton. Nordisk Betong, 4-10.

CLAUSEN, F.L. (1982). A geostatistical study of the uranium deposit at Kvanefjeld, The Ilímaussaq intrusion, South Greenland. Risø-R-468, 289 pp.

CULOT, M.V.J., OLSON, H.G. and SCHIAGER, K.J. (1976). Effective diffusion coefficient of radon in concrete, theory and method for field measurements. Health Phys. 30, 263-270.

DICKSON, B.L., CHRISTIANSEN, E.M. and LØVBORG, L. (1982). Reference materials for calibration of laboratory gamma-ray analyses. Uranium exploration methods (OECD, Paris) 687-698.

FULTON, F.S. (1964). Concrete technology (The Portland Cement Institute, Johannesburg).

GRASTY, R.L., BRISTOW, Q., CAMERON, G.W., DYCK, W., GRANT, J.A. and KILLEEN, P.G. (1982). Primary calibration of a laboratory gamma-ray spectrometer for the measurement of potassium, uranium and thorium. Uranium exploration methods (OECD, Paris) 699-712.

IAEA (1976). Radiometric reporting methods and calibration in uranium exploration. Technical Report Series No. 174 (International Atomic Energy Agency, Vienna), 57 pp.

KIRKEGAARD, P. and LØVBORG, L. (1979). Program system for computation of the terrestrial gamma-radiation field. Risø-R-392, 31 pp.

KOGAN, R.M., NAZAROV, I.M. and FRIDMAN, Sh.D. (1969). Osnovy Gamma-Spektrometrii Prirodnykh Sred (Gamma Spectrometry of Natural Environments and Formations). Atomizdat, Moskva. (English translation by Israel Program for Scientific Translations, Jerusalem 1971).

KUNZENDORF, H., LØVBORG, L. and CHRISTIANSEN, E.M. (1980). Automated uranium analysis by delayed-neutron counting. Risø-R-429, 38 pp.

LØVBORG, L., WOLLENBERG, H., ROSE-HANSEN, J. and NIELSEN, B.L. (1972). Drill core scanning for radioelements by gamma-ray spectrometry. Geophys. 37, 675-693.

LØVBORG, L., KIRKEGAARD, P. and CHRISTIANSEN, E.M. (1976). Design of NaI(Tl) scintillation detectors for use in gamma-ray surveys of geological sources. Exploration for uranium ore deposits (International Atomic Energy Agency, Vienna) 127-148.

LØVBORG, L., BØTTER-JENSEN, L. and KIRKEGAARD, P. (1978). Experiences with concrete sources for radiometric field instruments. Geophys. 43, 543-549.

LØVBORG, L., CHRISTIANSEN, E.M., BØTTER-JENSEN, L. and KIRKEGAARD, P. (1981). Pad facility for the calibration of gamma-ray measurements on rocks. Risø-R-454, 43 pp.

LØVBORG, L. (1982). Error analysis of calibration and field trials with spectrometers and counters. Uranium exploration methods (OECD, Paris) 671-680.

MAKOVICKY, M., MAKOVICKY, E., NIELSEN, B.L., KARUP-MØLLER, S. and SØRENSEN, E. (1980). Mineralogical, radiographic and uranium leaching studies on the uranium ore from Kvanefjeld, Ilímaussaq complex, South Greenland. Risø-R-416, 186 pp.

MATHEWS, M.A. and KOSANKE, K.L. (1978). Gross gamma-ray calibration blocks. GJBX-59 (78), 89 pp.

NCRP (1978). A handbook of radioactivity measurements procedures. Report No. 58 (National Council of Radiation Protection and Measurements, Washington, D.C.) p. 306 ff.

NEVILLE, A.M. (1977). Properties of concrete (Pitman Paperbacks, London).

NIELSEN, B.L. (1981). Exploration of the Kvanefjeld uranium deposit, Ilímaussaq intrusion, South Greenland. Uranium exploration case histories (International Atomic Energy Agency, Vienna) 353-388.

OECD (1981). Reporting and calibration of total-count gamma radiation measurements. Newsletter on R&D in uranium exploration techniques, No. 3 (OECD Nuclear Energy Agency, Paris) 16-19.

RIXOM, M.R. (1978). Chemical admixtures for concrete (Wiley & Sons, New York).

SØRENSEN, H., ROSE-HANSEN, J., NIELSEN, B.L., LØVBORG, L., SØRENSEN, E. and LUNDGAARD, T. (1974). The uranium deposit at Kvanefjeld, the Ilímaussaq intrusion, South Greenland. Rapp. Grønlands geol. Unders. 60, 54 pp.

TANNER, A.B. (1964). Radon migration in the ground: A review. The natural radiation environment (University of Chicago Press, Chicago) 161-190.

TANNER, A.B. (1980). Radon migration in the ground: A supplementary review. Natural radiation environment III, vol. 1 (U.S. Department of Energy, Springfield) 5-56.

TROXELL, G.E., DAVIS, H.E. and KELLY, J.W. (1968). Composition and properties of concrete (McGraw-Hill, New York).

APPENDIX A

REVISED RADIOELEMENT CONTENTS FOR THE SPECTROMETER CALIBRATION SOURCES UT-1 TO U-1

The in-situ radioelement contents of the six sources UT-1 to U-1 in Fig. 3 were originally estimated by gamma-ray counting of sealed sample material and the use of a moisture-correction factor of 1.06 (Løvborg et al., 1981). Since 1980 the sources have been repeatedly monitored with a GR-410 spectrometer as part of an IAEA-sponsored intercomparison of spectrometer calibration facilities in a number of countries (Løvborg, 1982). Calibration data for the GR-410 recorded with facilities in Canada, Finland, Sweden, and USA provided the new estimate for the Risø sources shown in Table 16. The most significant change with respect to the original estimate is a 14% reduction of the eU contents of the sources UT-1 and UT-2. This result suggests a fractional radon loss of the same order of magnitude; it is supported by the detection of emanation from samples of the source materials (Table 6). The large amount of monitoring data avail-

Table 16. Estimated in-situ radioelement concentrations for the spectrometer calibration sources at Risø.

Source	% K	ppm eU	ppm Th
UT-1	1.33 ± 0.05	48.7 ± 1.6	144 ± 4
UT-2	1.24 ± 0.02	16.7 ± 0.5	50.4 ± 1.1
K-1	1.03 ± 0.01	0.29 ± 0.04	2.3 ± 0.1
K-2	6.73 ± 0.08	4.19 ± 0.09	1.8 ± 0.1
T-1	0.73 ± 0.06	8.0 ± 0.5	150 ± 2
U-1	0.91 ± 0.05	148 ± 24	1.9 ± 0.5

able for the sources shows that the diminished radon contents of UT-1 and UT-2 are permanent. U-1, on the other hand has a seasonal emanation pattern (Løvborg, et al. 1978) and recovers its equilibrium content of radon in the winter when the supply of pore water is greatest.

Table 16 has been adopted as a list of most probable in-situ radioelement concentrations. This revision changes the uranium equivalents recorded in previous total-count experiments with the sources. (Løvborg et al. 1981). The experimental Ur correspondents of 1 ppm Th and 1% K reported in Table 11 are based on the revised reference concentrations and the single determinations presented in Tables 17 and 18.

Table 17. Experimental uranium equivalents recorded with 1 1/2 x 1 in. scintillation detector.

Threshold energy (keV)	Uranium equivalent (Ur)	
	1 ppm Th	1% K
30	0.36 ± 0.01	0.92 ± 0.04
60	0.36 ± 0.01	0.95 ± 0.04
90	0.37 ± 0.01	1.03 ± 0.04
120	0.37 ± 0.01	1.10 ± 0.05
150	0.37 ± 0.01	1.16 ± 0.05

Table 18. Experimental uranium equivalents recorded with 2 x 2 in. scintillation detector.

Threshold energy (keV)	Uranium equivalent (Ur)	
	1 ppm Th	1% K
50	0.36 ± 0.01	1.16 ± 0.05
100	0.37 ± 0.01	1.33 ± 0.05
150	0.37 ± 0.01	1.44 ± 0.05
200	0.38 ± 0.01	1.59 ± 0.06

APPENDIX B

ACCURACY PROVIDED BY THE LABORATORY COUNTING STANDARDS

The estimated block grades indirectly depend on U and Th reference materials originating from the New Brunswick Laboratory of the U.S. Department of Energy. Calibration results obtained with six thorium and five uranium NBL counting standards are shown in Tables 19 and 20. The eU contents of the uranium standards are based on the certified U concentrations plus a stated content of 3.44×10^{-7} g Ra per g U. This radium content is slightly greater than that produced by one gram of uranium in equilibrium and corresponds to a radiometric factor of 1.019 ppm eU per ppm U. The use of such a factor is perhaps not relevant since the uncertainty of the Ra/U ratio is not specified in the NBL certificates (Dickson et al., 1982). Tables 19 and 20 suggest that

Table 19. Laboratory thorium counting sensitivities recorded with NBL reference materials.

NBL reference material	Thorium concentration (ppm Th)	Counts/s per g Th (2.41-2.81 MeV)
80	1010 ± 15	61.4 ± 1.0
80A	1005 ± 5	61.5 ± 0.6
83A	101 ± 1.5	61.6 ± 1.0
107	1000 ± 20	64.1 ± 1.3
108	520 ± 5	61.6 ± 0.8
109	104 ± 1.5	63.6 ± 1.1
Weighted mean		61.9
Coefficient of variation		1.6%

Table 20. Laboratory uranium counting sensitivities recorded with NBL reference materials.

NBL reference material	Equivalent uranium concentration (ppm eU)	Counts/s per g eU (1.66-1.86 MeV)
74	1019 ± 20	166.5 ± 3.4
74A	1060 ± 10	164.7 ± 1.9
76B	103 ± 1	172.9 ± 2.1
102	1029 ± 5	170.3 ± 2.1
104	105 ± 2	162.8 ± 3.4
Weighted mean		168.2
Coefficient of variation		2.4%

the systematic assay error associated with calibrations against NBL standards amounts to about 1.5% for Th and 2% for eU. These accuracies were assumed in assigning uncertainties to the assay results in Tables 2 and 7. Improved radiometric accuracies may be obtained with counting standards prepared from an old thorium salt and radium chloride (Grasty et al., 1982).

APPENDIX C

ASSAY OF RADON EMANATION USING REPEATED GAMMA-RAY COUNTING

Emanation power can be estimated by sealing the material and executing an initial and a final count of the gamma-rays emitted from the sample (Austin, 1975). The method used for recording the emanation data in Table 6 is a slightly refined version of the technique and is based on repetitive activity measurements over a four-week period.

Figure 16 shows the time dependence of ^{222}Rn and ^{214}Bi for material with an induced radon loss of 100% just before sealing a sample. Over the first few hours ^{214}Bi decays to less than 3% of its previous equilibrium concentration. Six hours after the sealing ^{214}Bi is in transient equilibrium with freshly formed ^{222}Rn and follows the exponential growth of the latter with a time lag of 1.20 hours. The time lag is a consequence of the decay constants in the system

$$^{222}Rn \xrightarrow[3.82d]{} {}^{218}Po \xrightarrow[3.05m]{} {}^{214}Pb \xrightarrow[26.8m]{} {}^{214}Bi \xrightarrow[19.5m]{} {}^{214}Po$$

By using the sealing time plus 1.20 hours as a new time reference, radon contained in unsealed material can be measured by extrapolating the ^{214}Bi growth curve to zero time. An additional extrapolation to infinite time furnishes the final equilibrium content of radon. The difference between the two levels is the initial radon loss.

Figure 17 shows the result of fitting exponential curves with the decay constant of ^{222}Rn (0.1813 d^{-1}) to five determinations of the eU content in sealed samples of source material U-1. Curve A is for dry material and indicates an emanation power of 5%. Curve B provides the radon loss invoked by heating a

moistened sample to 60°C (11%, Table 6). Repeat trials have demonstrated that emanation down to a few percent can be detected with the method.

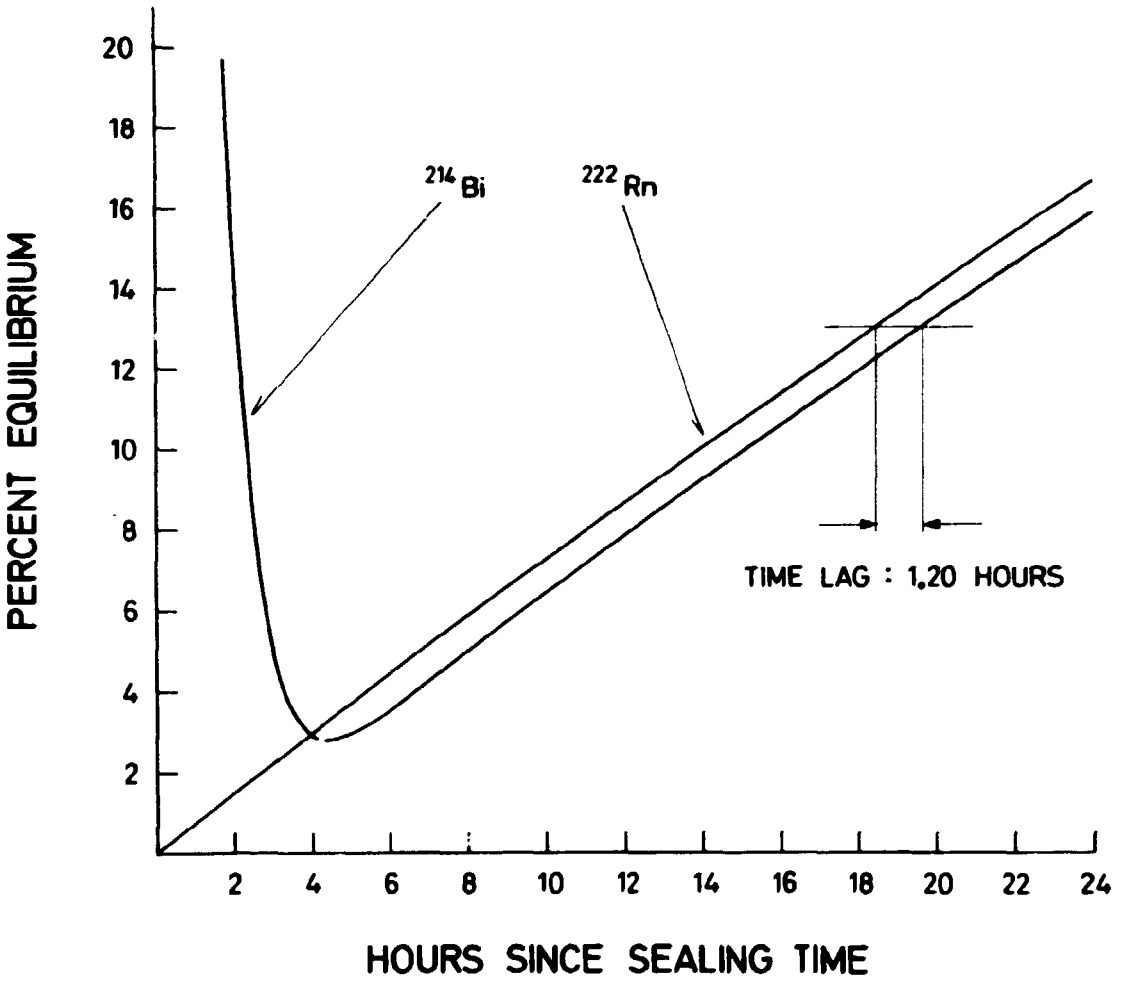

Fig. 16. Time dependence of ^{222}Rn and ^{214}Bi in sealed sample depleted of its ^{222}Rn at t=0.

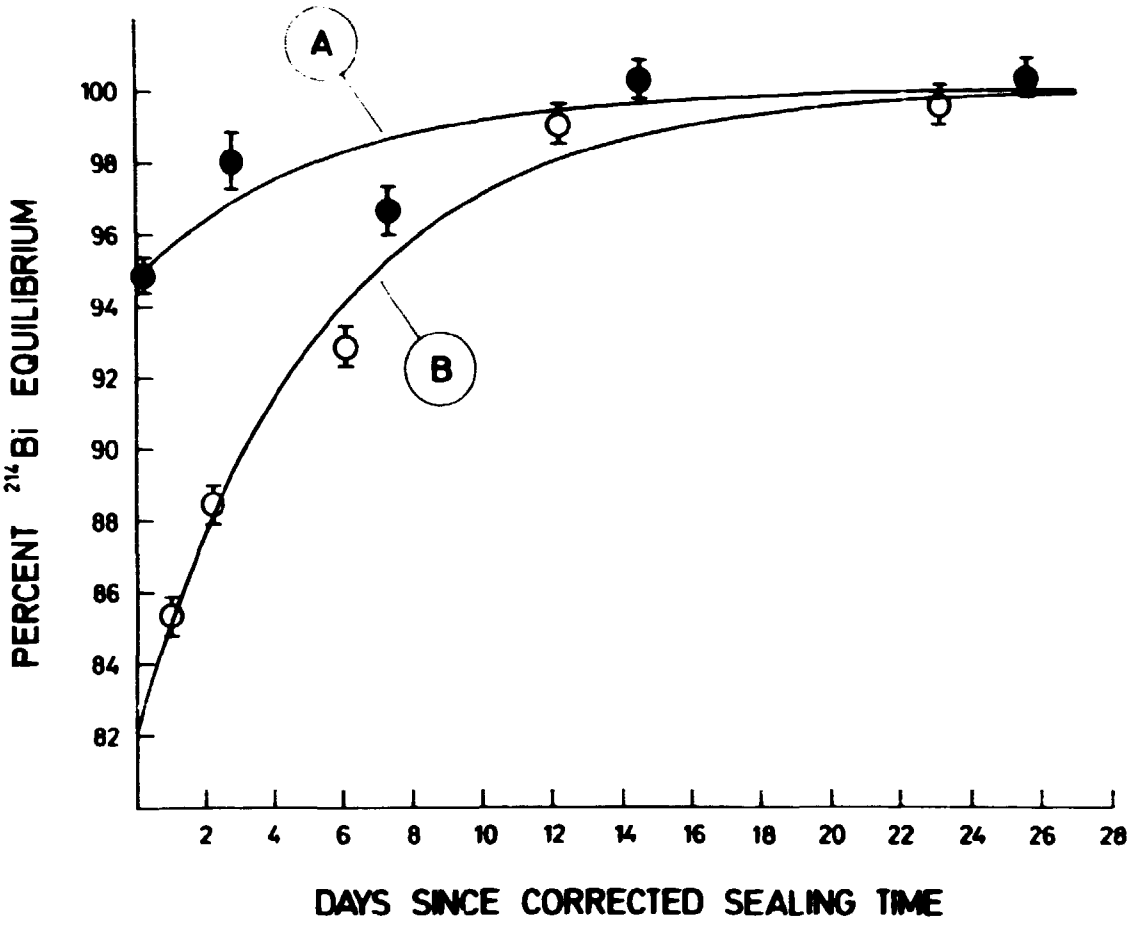

Fig. 17. Experimental determination of radon emanation from the exponential growth of ^{214}Bi in sealed samples of source material U-1. A: Dry material. B: Moistened material heated to 60°C for two days.

Sales distributors:
Jul. Gjellerup, Sølvgade 87,
DK-1307 Copenhagen K, Denmark

Available on exchange from:
Risø Library, Risø National Laboratory,
P.O.Box 49, DK-4000 Roskilde, Denmark

ISBN 87-550-0958-1
ISSN 0106-2840